

weekly report

Harel Yona, Rachel Finkelshtein

Contents

I. Introduction	1
II. Methods	1
A. Experimental Setup	1
B. Uncertainties	1
III. Double Polarizer	1
IV. Triple Polarizers	2
V. Wave Plate	2
A. Half-Wave Plate	2
B. Quarter Wave Plate	3
VI. Refraction	4
A. Fresnel equations	4
B. Brewster's Angle	4

I Introduction

In this experiment, we systematically investigated the interaction of polarized laser light with a variety of optical components, including polarizers, wave plates, and dielectric interfaces.

A foundational principle in the study of polarized light is Malus' Law, which quantifies how the intensity of linearly polarized light changes as it passes through a polarizing filter. Mathematically, Malus' Law is expressed as

$$I = I_0 \cos^2(\theta), \quad (1)$$

where I_0 is the incident light intensity and θ is the angle between the light's initial polarization direction and the transmission axis of the polarizer. This relationship predicts that the transmitted intensity varies as the square of the cosine of the relative angle, reaching a maximum when the polarizer is aligned ($\theta = 0$) and dropping to zero when it is crossed ($\theta = 90^\circ$).

Our primary aim was to explore how these elements influence the intensity and polarization state of a laser beam. Using a setup comprising polarizers, a photomultiplier, and birefringent wave plates, we verified theoretical predictions such as Malus' Law and the behavior of light through multiple polarizers. We extended this analysis to polarization-altering elements, including half- and quarter-wave plates, and evaluated their impact on transmitted light intensity and polarization.

Additionally, we investigated Fresnel reflection effects at a PMMA-air interface, including the identification of Brewster's angle — a key phenomenon in

polarization-dependent reflectance. The experimental results were compared with theoretical models.

II Methods

A Experimental Setup

The experimental setup consists of a laser source, a photomultiplier, set of polarizers and 2 wave plates. The photomultiplier detects the intensity of the laser beam and converts it into an electrical signal.

B Uncertainties

There are two sources of uncertainty to consider:

- **Emitted Intensity** — The laser's intensity is not constant, but fluctuates around a mean value. This uncertainty is quantified as the standard deviation of each measurement.
- **Angle** — All components were placed manually, which introduces angular imprecision. This uncertainty is estimated as half the smallest division on the calibration scale, i.e., 0.5° .

III Double Polarizer

Two polarizers were arranged in series: the first produced linearly polarized light, and the second was used to measure the transmitted intensity as its axis was rotated through various angles.

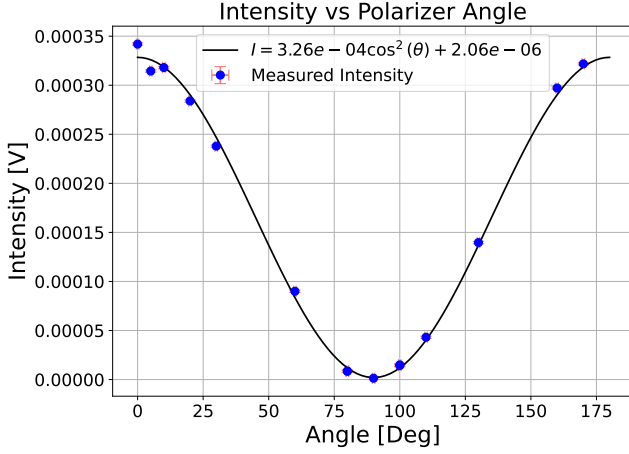


Figure 1: Measured light intensity at various angles (blue dots), with red error bars indicating uncertainties in both angle and intensity. The black curve represents the fitted function of the form $A \cos^2 \theta + B$.

As shown in Figure 1, the experimental data closely follows the theoretical curve. The fitted parameters are:

$$A = (3.26 \pm 0.12) \times 10^{-4} \frac{W}{m^2} \quad (2)$$

$$B = (2.06 \pm 0.07) \times 10^{-6} \frac{W}{m^2} \quad (3)$$

Parameter A represents the initial intensity according to the fitted function. The measured value of I_0 (the intensity of the strongest measurement at 0°) is $(3.42 \pm 0.03) \times 10^{-4} \frac{W}{m^2}$, which deviates by approximately 4.77% from the fitted value

IV Triple Polarizers

Following the previous section, we now explore the intensity of a laser beam passing through three polarizers — that is, adding a second polarizer at an angle θ' relative to the first. The expression for the transmitted intensity is given by:

$$I = I_0 \cos^2(\theta) \cos^2(\theta') \quad (4)$$

To simplify this expression, we consider the case where the third polarizer is placed perpendicular to the original polarization direction, such that $\theta' = 90^\circ - \theta$. Substituting this into the equation yields:

$$I = I_0 \cos^2(\theta) \cos^2(90^\circ - \theta) = I_0 \sin^2(\theta) \cos^2(\theta) \quad (5)$$

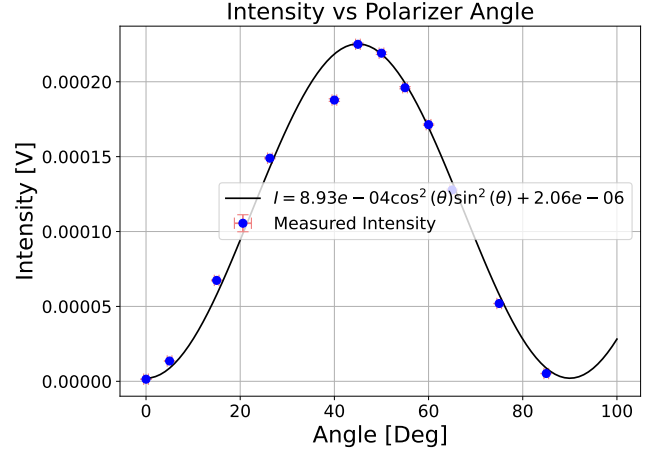


Figure 2: Measured light intensity at various angles (blue dots), with red error bars indicating uncertainties in both angle and intensity. The black curve represents the fitted function of the form $A \sin^2 \theta \cos^2 \theta + B$.

Excluding a single outlier, Figure 2 shows strong agreement with the theoretical prediction based on Malus' Law. The anomalous data point resulted from a brief accidental obstruction of the laser beam, which temporarily reduced the measured intensity and thus lowered the average intensity for that specific angle.

V Wave Plate

A wave plate is an optical component which alter the polarization of the state of the light traveling through it. In our experiment we aim to study the light's intensity traveling through two commonly used wave plates: half and quarter.

A Half-Wave Plate

In this part of the experiment, we began by measuring the transmitted light intensity through two polarizers and an half wave plate. The first polarizer was fixed at a reference orientation, the wave plate was placed at a specific angle with respect to the optical axis of the first polarizer. We then recorded the transmitted intensity at various angles using the second polarizer.

This process was repeated twice: first with the wave plate oriented at 0° , and then at 30° relative to the optical axis. The first is a simple case of double polarizers, thus, follows the standard Malus' Law. The expected behavior of the second is described by a modified form of Malus' Law. A half-wave plate rotates the polarization direction of incident light by 2θ , where θ is the angle between the incoming polarization and the optical axis of

the wave plate. Therefore, the transmitted intensity is given by:

$$I = I_0 \cos^2(\theta - \theta_0 - \phi) \quad (6)$$

where θ_0 is the angle of the initial position and ϕ is the phase shift which expected to be 60° .

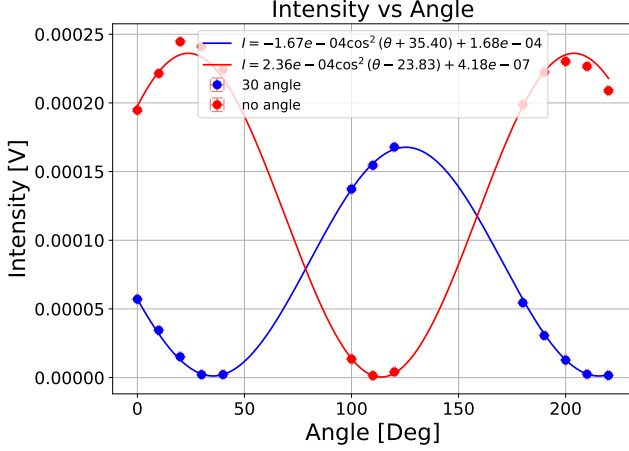


Figure 3: Measured light intensity as a function of the half-wave plate angle. The red points represent the setup with two aligned polarizers, while the blue points include a half-wave plate fixed at 30° relative to the first polarizer. Error bars reflect uncertainties in both angle and intensity. Smooth curves represent best-fit \cos^2 models based on Eq. 6.

Fitting the measurements of 0° wave plate with the standard form of Malus' Law results with angle phase $\theta_0 = 23.8^\circ \pm 0.8^\circ$. The fit parameters for the half wave plate with 30° are:

$$A = (1.67 \pm 0.04) \times 10^{-4} \frac{W}{m^2} \quad (7)$$

$$B = 59.2^\circ \pm 0.9^\circ \quad (8)$$

$$C = (1.6 \pm 0.1) \times 10^{-4} \frac{W}{m^2} \quad (9)$$

As shown in Figure 3, both datasets display the expected periodic behavior, consistent with the cosine-squared model. The fitted curves accurately capture key features such as amplitude, phase shift, and baseline offset.

The intensity values in the configuration including the half-wave plate (blue) are consistently lower than those in the two-polarizer setup (red). This reduction is attributed to the physical presence of the wave plate: as light passes through its birefringent material, a fraction is absorbed, leading to a measurable decrease in the total transmitted intensity. Additionally, a rotation of the wave plate by 30° resulted in a phase shift of $59.2^\circ \pm 0.9^\circ$, which closely matches the expected value of 60° .

B Quarter Wave Plate

In this setup, we employed the same configuration as described previously, with the exception that the half-wave plate was replaced by a quarter-wave plate. The quarter-wave plate introduces a phase shift of $\frac{\pi}{2}$ between the orthogonal polarization components of the incident beam, thereby converting linearly polarized light into elliptically polarized light.

A special case arises when the quarter-wave plate is oriented at 45° with respect to the polarization axis. In this configuration, the electric field components along the fast and slow axes are equal in amplitude, and the introduced phase shift of $\frac{\pi}{2}$ results in circular polarization.

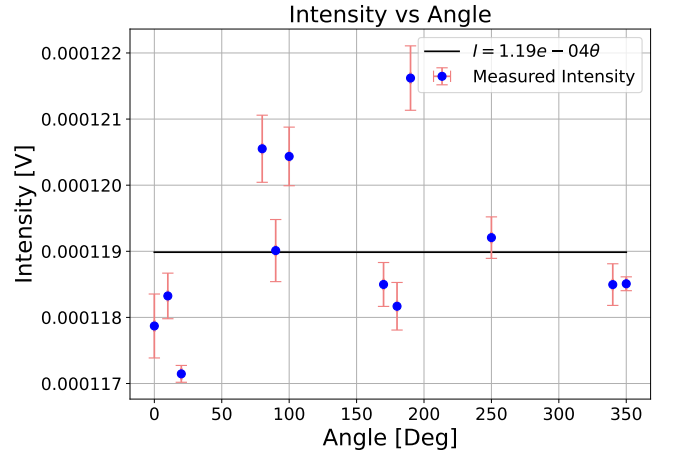


Figure 4: Measured light intensity as a function of the quarter-wave plate angle. Blue points represent the data, and the black line is an average of the measured intensities.

A constant line of the average measured intensities of the form $I = A$, the fit results in:

$$A = 1.189864166 \pm 0.000000001 \times 10^{-4} \frac{W}{m^2} \quad (10)$$

Perfect circular polarization is characterized by a constant intensity independent of the rotation angle. As can be seen, this condition is not fully met in our measurement. However, we achieved a good approximation, as indicated by the low uncertainty of the fit coefficient. The primary reason for this deviation is the sensitivity of circular polarization to the exact orientation and properties of the optical elements; even slight mismatches from the ideal conditions can disturb the polarization state.

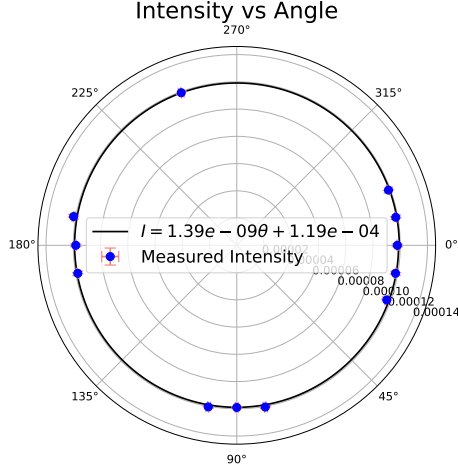


Figure 5: Polar plot of the measured intensity as a function of the quarter-wave plate angle. An ideally circular polarization would yield a perfect circle in such a plot; the slight deviation illustrates small imperfections in the setup.

VI Refraction

A Fresnel equations

In this section, we aim to explore the characteristics of refraction. A polarized laser beam was directed into a PMMA medium, and its vertical and horizontal polarization components were analyzed at various angles of incidence. According to the Fresnel equations, the reflectance of each polarization component can be expressed as follows:

$$r_s = \frac{n_{\text{in}} \cos \theta - n_{\text{out}} \sqrt{1 - \left(\frac{n_{\text{in}}}{n_{\text{out}}} \cos \theta\right)^2}}{n_{\text{in}} \cos \theta + n_{\text{out}} \sqrt{1 - \left(\frac{n_{\text{in}}}{n_{\text{out}}} \cos \theta\right)^2}} \quad (11)$$

$$r_p = \frac{n_{\text{out}} \cos \theta - n_{\text{in}} \sqrt{1 - \left(\frac{n_{\text{in}}}{n_{\text{out}}} \cos \theta\right)^2}}{n_{\text{out}} \cos \theta + n_{\text{in}} \sqrt{1 - \left(\frac{n_{\text{in}}}{n_{\text{out}}} \cos \theta\right)^2}} \quad (12)$$

where n_{in} and n_{out} are the refractive indices of the initial and second media, respectively, and θ is the angle of incidence.

B Brewster's Angle

Fresnel equations (Eq. 11) predict that for any interface between two media with different refractive indices, there exists a specific angle of incidence — called Brewster's angle, θ_b — at which the reflectance of p -polarized

light becomes zero. This occurs when the reflected and refracted rays are perpendicular, and is given by:

$$\theta_b = \arctan \left(\frac{n_{\text{out}}}{n_{\text{in}}} \right) \quad (13)$$

For a PMMA–air interface, where $n_{\text{in}} = 1$ (air) and $n_{\text{out}} = 1.49$ (PMMA), the theoretical Brewster angle is:

$$\theta_b^{\text{theoretical}} = \arctan(1.49) \approx 56.13^\circ \quad (14)$$

To test this prediction, we measured the reflected intensities of both p -polarized (horizontal) and s -polarized (vertical) light as a function of the incidence angle. The data was fitted using Fresnel's equations, with the best-fit Brewster angle matching the theoretical value:

$$\theta_b^{\text{fit}} = 56.13^\circ \quad (15)$$

Figure 6 shows the full angular range, where we observe the decreasing trend in the p -component and a corresponding increase in the s -component.

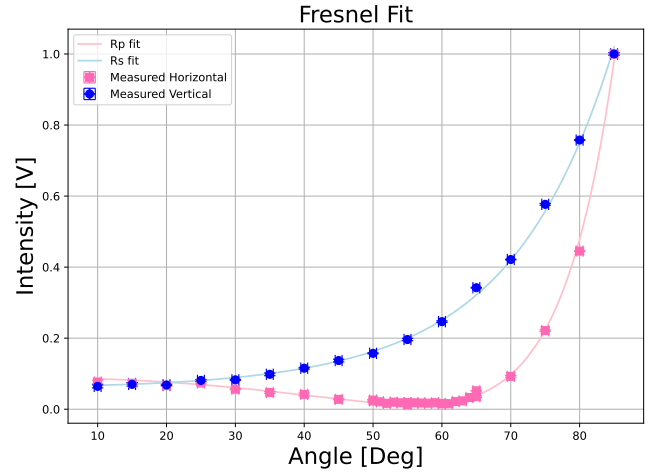


Figure 6: Reflected intensity as a function of incident angle for both horizontal (p -polarized) and vertical (s -polarized) components. The fitted curves are based on Fresnel's equations.

To more accurately identify the Brewster angle, we performed a high-resolution scan around the predicted value. The results are shown in Figure 7, where the p -component shows a sharp minimum near 56.13° . Fresnel coefficients computed from the fit support this: for example, at 56° , $R_p \approx 0$ and $R_s \approx 0.143$, consistent with theory.

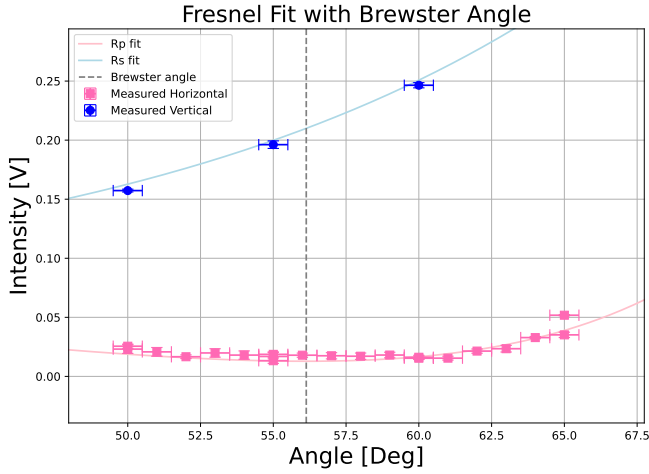


Figure 7: Zoomed-in measurement near the Brewster angle. The horizontal (p) component exhibits a pronounced dip at 56.13° , while the vertical (s) component continues to increase.

Fit parameters for the reflected intensity curves were

obtained by matching the theoretical Fresnel reflection coefficients to the experimental intensity data. The **scale** parameter accounts for the conversion between reflection coefficient and measured voltage, while the **offset** represents a constant background signal from the detector. The fitted curves show good agreement with the experimental points, confirming the validity of the Fresnel-based model:

- Vertical (s): scale = 1.381, offset = 0.0116
- Horizontal (p): scale = 1.962, offset = 0.0128

The uncertainties in the fitted parameters were found to be approximately three orders of magnitude smaller than the parameter values themselves; therefore, we did not include them here, as the fit visibly provides excellent agreement with the experimental data.

This experiment highlights the distinct behaviors of polarized light at an interface, demonstrating the zero reflection condition of p polarized light at the Brewster angle. Such properties have practical applications in the design of antireflective coatings and in controlling polarization in optical systems.